Kinetic Study of the Reactions of Br with HO₂ and DO₂

Yuri Bedjanian,* Véronique Riffault, Georges Le Bras, and Gilles Poulet[†]

Laboratoire de Combustion et Systèmes Réactifs, CNRS and Université d'Orléans,
45071 Orléans Cedex 2, France

The kinetics of the reactions of Br atoms with HO₂ and DO₂ radicals, Br + HO₂ → HBr + O₂ (1), and Br + DO₂ → DBr + O₂ (3), have been studied by the mass spectrometric discharge-flow method at temperatures between 230 and 355 K and at a total pressure of 1 Torr of helium. The rate coefficients measured under pseudo-first-order conditions in excess Br yield the following Arrhenius expressions: $k_1 = (4.9 \pm 0.7) \times 10^{-12} \exp[-(310 \pm 40)/T]$ and $k_3 = (1.9 \pm 0.4) \times 10^{-12} \exp[-(540 \pm 60)/T]$ cm³ molecule⁻¹ s⁻¹ (uncertainties are 2σ). The k_3 value is measured for the first time and that of k_1 is compared with those from previous studies.

Introduction

The reaction of Br atoms with HO₂ radicals has been recognized as one of the important removal processes for active bromine species (Br + BrO) in the stratosphere (e.g., ref 1):

$$Br + HO_2 \rightarrow HBr + O_2 \qquad (1)$$
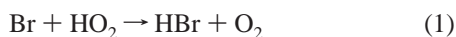
Three room-temperature measurements of the reaction rate constant have been reported previously.[2–4] The discharge flow reactor was used in these three studies. The first measurement by Posey et al.[2] using mass spectrometric detection led to $k_1 = (2.2 \pm 1.1) \times 10^{-13}$ cm³ molecule⁻¹ s⁻¹. A significantly higher value of $(7.6 \pm 0.9) \times 10^{-13}$ cm³ molecule⁻¹ s⁻¹ was measured by Poulet et al.,[3] employing laser-induced fluorescence and mass spectrometry techniques. In the same group, reaction 1 was revisited with the electron paramagnetic resonance (EPR) technique,[4] leading to $k_1 = (1.5 \pm 0.2) \times 10^{-12}$ cm³ molecule⁻¹ s⁻¹. Surprisingly, despite the importance of the reaction 1 in atmospheric bromine chemistry, this reaction has never been studied at stratospheric temperatures. In the unique temperature-dependent study of Toohey et al.,[5] where laser magnetic resonance and resonance fluorescence methods were used for the respective detection of HO₂ and Br, the rate constant of reaction 1 was measured at temperatures between 260 and 390 K: $k_1 = (1.4 \pm 0.2) \times 10^{-11} \exp[(-590 \pm 140)/T]$ cm³ molecule⁻¹ s⁻¹ with $k_1 = (1.98 \pm 0.05) \times 10^{-12}$ cm³ molecule⁻¹ s⁻¹ at $T = 298$ K. Current evaluations of the kinetic data for atmospheric modeling[6,7] recommend a temperature dependence of k_1 on the basis of the results of Toohey et al. To better quantify the HBr production rate from reaction 1, a direct measurement of k_1 under stratospheric temperatures is clearly needed.

Another motivation of this work is the interaction of reaction 1 with the reaction between OH and BrO radicals, which is currently under study in this laboratory:

$$OH + BrO \rightarrow HO_2 + Br \qquad (2a)$$
$$\rightarrow HBr + O_2 \qquad (2b)$$

The potential occurrence of channel (2b) is of great importance for the stratospheric bromine partitioning.[8,9] Hence, the experimental determination of the branching ratio for channel (2b) is required. Since this branching ratio is expected to be very low (a few percent), the secondary and side processes involving reactants and products of reaction 1 as well as the species used to produce OH and BrO radicals cannot be neglected and must be well characterized. The reaction of Br with HO₂ leading to HBr formation is one of these processes. The detection of small yields of HBr from OH + BrO reaction is rather challenging, because non-negligible residual concentrations of HBr are known to be present in bromine-containing chemical systems in the laboratory. In this respect, the reaction OD + BrO, the isotopic analogue of reaction 2, seems to be better adapted for the determination of the DBr yield. However, in this case, the rate constant data on the relevant reactions of OD and DO₂ radicals (which are very scarce) are needed. In previous papers from this laboratory, the kinetic data for reactions OH(OD) + OH(OD),[10] OH(OD) + Br₂,[11] and OH(OD) + HBr(DBr)[12] have been reported. The present work reports the measurements of the rate constants for reactions 1 and 3 over the temperature range 230–355 K:

$$Br + DO_2 \rightarrow DBr + O_2 \qquad (3)$$
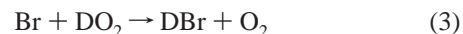
Experimental Section

Experiments were carried out in a discharge flow reactor using a modulated molecular beam mass spectrometer as the detection method. The main reactor, shown in Figure 1 along with the movable injector for the reactants, consisted of a Pyrex tube (45 cm length and 2.4 cm i.d.) with a jacket for the thermostated liquid circulation (water or ethanol). The walls of the reactor as well as of the injector were coated with halocarbon wax in order to minimize the heterogeneous loss of active species. All experiments were conducted at 1 Torr total pressure, helium being used as the carrier gas.

* Corresponding author (E-mail: bedjanian@cnrs-orleans.fr).
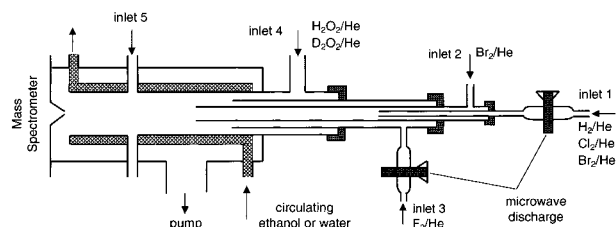† Present address: CNRS−LPCE (Laboratoire de Physique et Chimie de l'Environnement), Orléans.

574 *J. Phys. Chem. A, Vol. 105, No. 3, 2001*

Bedjanian et al.

Figure 1. Diagram of the apparatus used.

Three different methods were used to produce Br atoms (either the microwave discharge of Br_2/He mixtures or the fast reactions of H or Cl atoms with an excess concentration of Br_2):

$$H + Br_2 \rightarrow Br + HBr \qquad (4)$$

$$k_4 = 6.7 \times 10^{-10} \exp(-670/T) \, cm^3 \, molecule^{-1} \, s^{-1} \, {}^{13}$$

$$Cl + Br_2 \rightarrow Br + BrCl \qquad (5)$$

$$k_5 = 2.3 \times 10^{-10} \exp(-135/T) \, cm^3 \, molecule^{-1} \, s^{-1} \, {}^{14}$$

In all experiments, Br atoms were introduced in the reactor through the central tube of the movable injector. H and Cl atoms were formed in the microwave discharge of H_2/He or Cl_2/He mixtures, respectively (inlet 1), and excess Br_2 was introduced through inlet 2. Br_2 was always present in the reactor at concentrations $(3-5) \times 10^{13}$ molecule cm^{-3}. The fast reaction of fluorine atoms with H_2O_2 (inlet 4) was used as the source of HO_2 radicals, F atoms being produced in the microwave discharge of F_2/He mixture (inlet 3):

$$F + H_2O_2 \rightarrow HO_2 + HF \qquad (6)$$
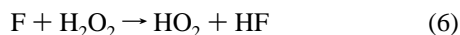
$$k_6 = 5.0 \times 10^{-11} \, cm^3 \, molecule^{-1} \, s^{-1} \, (T = 300 \, K)^{15}$$

To reduce F atom reactions with glass surface inside the microwave cavity, a ceramic (Al_2O_3) tube was inserted in this part of the injector. Similarly, the reaction of F atoms with D_2O_2 was used to produce DO_2 radicals:

$$F + D_2O_2 \rightarrow DO_2 + DF \qquad (7)$$

H_2O_2 and D_2O_2 (in solution in H_2O and D_2O, respectively) were always used in excess over F atoms. This source of HO_2(DO_2) radicals is known to produce other active species. In particular, OH(OD) radicals can be formed in reaction of F atoms with H_2O (D_2O):

$$F + H_2O \rightarrow OH + HF \qquad (8)$$

$$k_8 = 1.4 \times 10^{-11} \exp[(0 \pm 200)/T] \, cm^3 \, molecule^{-1} \, s^{-1} \, {}^6$$

$$F + D_2O \rightarrow OD + DF \qquad (9)$$

Other active species which can enter the main reaction zone of the reactor are O atoms, either from the F_2 discharge or from the secondary reaction $F + OH \rightarrow O + HF$. In this respect, the advantage of the chemical system used in the present study was the presence of Br_2 in the reactor. Br_2 reacts with the above-mentioned OH and O species but it is unreactive with HO_2 radicals. Consequently, it will deplete any of the secondary radicals that remain after the initial $F + H_2O_2(H_2O)$ reaction:

$$OH + Br_2 \rightarrow Br + HOBr \qquad (10)$$

$$k_{10} = 1.8 \times 10^{-11} \exp(235/T) \, cm^3 \, molecule^{-1} \, s^{-1} \, {}^{11}$$

$$OD + Br_2 \rightarrow Br + DOBr \qquad (11)$$

$$k_{11} = 1.9 \times 10^{-11} \exp(220/T) \, cm^3 \, molecule^{-1} \, s^{-1} \, {}^{11}$$

$$O + Br_2 \rightarrow BrO + Br \qquad (12)$$

$$k_{12} = 1.8 \times 10^{-11} \exp(40/T) \, cm^3 \, molecule^{-1} \, s^{-1} \, {}^{16}$$

$$F + Br_2 \rightarrow FBr + Br \qquad (13)$$

$$k_{13} = 2.2 \times 10^{-10} \, cm^3 \, molecule^{-1} \, s^{-1} \, (T = 300 \, K)^{17}$$

The products of the Br_2 reactions can be easily measured, using the mass spectrometric detection of HOBr(DOBr), BrO, and FBr. The BrO product can potentially interfere with kinetic measurements (via reactions 14 and 15), however, its concentration was found to be less than 10^{11} molecule cm^3 under the conditions of the present experiments and thus was too low to significantly influence the kinetics of HO_2(DO_2):

$$HO_2 + BrO \rightarrow HOBr + O_2 \qquad (14)$$
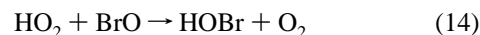
$$k_{14} = 9.4 \times 10^{-12} \exp(345/T) \, cm^3 \, molecule^{-1} \, s^{-1} \, {}^{18}$$

$$DO_2 + BrO \rightarrow DOBr + O_2 \qquad (15)$$
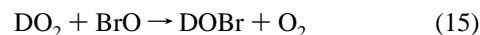
$$k_{15} = 3.9 \times 10^{-12} \exp(410/T) \, cm^3 \, molecule^{-1} \, s^{-1} \, {}^{18}$$

The HO_2 and DO_2 radicals were detected at their parent peaks at $m/e = 33$ (HO_2^+) and $m/e = 34$ (DO_2^+), respectively. These signals were always corrected for contributions from H_2O_2 and D_2O_2 due to their fragmentation in the ion source, which operated at $25-30$ eV. These corrections could be easily done by simultaneous detection of the signals from H_2O_2 at $m/e = 33$ and 34 ($m/e = 34$ and 36 for D_2O_2) and were around 10% of the signals corresponding to the initial concentrations of HO_2 and DO_2. HO_2 was also detected by chemical conversion with NO. Specifically, when NO is added at the end of the reactor (through inlet 5, located 5 cm upstream of the sampling cone), HO_2 is converted to NO_2 and can be detected at $m/e = 46$ as NO_2^+:

$$HO_2 + NO \rightarrow OH + NO_2 \qquad (16)$$
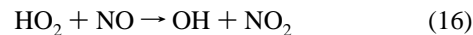
$$k_{16} = 3.5 \times 10^{-12} \exp(250/T) \, cm^3 \, molecule^{-1} \, s^{-1} \, {}^6$$

Reaction 16 leads to simultaneous production of OH radicals, which are rapidly scavenged by Br_2 (as mentioned above) through reaction 10, forming HOBr. Assuming a stoichiometric conversion of HO_2 to NO_2 and OH to HOBr, one has: $[HO_2] = [NO_2] = [HOBr]$. Figure 2 shows the pseudo-first-order plot measured at room temperature for the kinetics of HO_2 consumption in reaction with excess Br, using the different methods for the detection of HO_2. The experimental results obtained with the different approaches for the HO_2 detection are in excellent agreement. The detection of HO_2 as $HOBr^+$ could be complicated by the presence of background HOBr resulting from the reaction of OH impurity (present in the HO_2 source) with excess Br_2. However, this background level of HOBr was measured to be much lower than the initial concentration of HO_2: [HOBr] < 0.03 [HO_2]. Kinetic measurements at different temperatures have been conducted with direct HO_2 and DO_2 detection at m/e
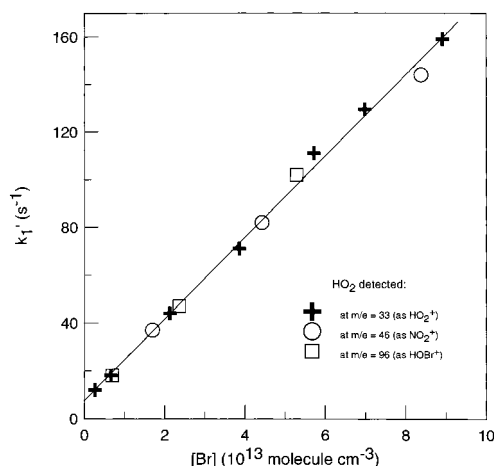
Reactions of Br with HO$_2$ and DO$_2$

J. Phys. Chem. A, Vol. 105, No. 3, 2001 **575**

Figure 2. Reaction Br + HO$_2$ → HBr + O$_2$: pseudo-first-order plot obtained from HO$_2$ decay kinetics in excess of Br atoms at $T = 297$ K using different methods of HO$_2$ detection (see text).

TABLE 1: Reaction Br + HO$_2$ → HBr + O$_2$: Experimental Conditions and Results

no./exp.[a]	T (K)	[Br] (10^{13} molecule cm^{-3})	$k_1{}^b$ (10^{-12} cm^3 molecule^{-1} s^{-1})	source of Br atoms
8	355	0.4–6.4	2.05 ± 0.24	H + Br$_2$
7	350	1.4–11.5	2.05 ± 0.28	Br$_2$ discharge
7	320	2.0–8.0	1.97 ± 0.29	H + Br$_2$
13	297	0.3–8.9	1.71 ± 0.20	H + Br$_2$
8	275	1.2–8.2	1.60 ± 0.21	H + Br$_2$
8	258	1.0–13.3	1.48 ± 0.18	Cl + Br$_2$
7	240	1.0–10.4	1.30 ± 0.18	Cl + Br$_2$
10	233	1.3–14.5	1.33 ± 0.17	Br$_2$ discharge
8	230	0.8–10.0	1.35 ± 0.18	Cl + Br$_2$

[a] Number of kinetic runs. [b] Quoted uncertainty represents 1σ + 10%.

2[H$_2$O] + 2[H$_2$O$_2$], and considering known concentrations of F atoms and H$_2$O, one could determine [H$_2$O$_2$]. In the present experiments the [H$_2$O$_2$]/[H$_2$O] ratio in the reactor was found to be around 1.5, which corresponds to a ≈90% H$_2$O$_2$/H$_2$O solution. The measurements of the absolute concentrations of H$_2$O and H$_2$O$_2$ were not necessary for the determination of the kinetic parameters in the present study. The above proposed calibration method has a methodical interest, although it seems to be rather complicated, especially if compared with the usually used calibration procedure based on vapor pressure measurements above the liquid solutions. However, the advantage of the radical titration method is that it allows direct measurements of H$_2$O$_2$ (H$_2$O) concentrations in the reactor and is independent of the conditions in the bubbled liquid solution (such as carrier gas flow rate, temperature, and sample concentration).

The purities of the gases used were as follows: He > 99.9995% (Alphagaz) was passed through liquid nitrogen traps; H$_2$ > 99.998% (Alphagaz); Cl$_2$ > 99% (Ucar); Br$_2$ > 99.99% (Aldrich); NO$_2$ > 99% (Alphagaz); and NO > 99% (Alphagaz), purified by trap-to trap distillation in order to remove NO$_2$ traces. A 70% H$_2$O$_2$ solution was purified to around 90% by continuously flowing helium through the bubbler with H$_2$O$_2$. The same procedure was employed for purification of D$_2$O$_2$, which was supplied as 30% solution in D$_2$O (ICON).

= 33 and 34, respectively. The absolute concentrations of HO$_2$ were measured using chemical conversion of HO$_2$ to NO$_2$ through reaction 16. To prevent possible HO$_2$ regeneration through reaction 17, the calibration was done with Br$_2$ present to scavenge OH:

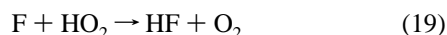$$OH + H_2O_2 \rightarrow HO_2 + H_2O \qquad (17)$$
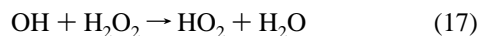
$$k_{17} = 2.9 \times 10^{-12} \exp(-160/T) \text{ cm}^3 \text{ molecule}^{-1} \text{ s}^{-1}\,[6]$$

A similar procedure was employed for the measurements of the absolute concentrations of DO$_2$ radicals. The concentrations of NO$_2$, as well as the concentrations of the other stable species used, were determined from the measurements of pressure drop rate in flasks containing mixtures of known dilution. The absolute concentrations of Br atoms could be found from the fraction of Br$_2$, either dissociated in the microwave discharge ([Br] = 2Δ[Br$_2$]) or consumed in reactions 4 or 5 with H and Cl, respectively ([Br] = Δ[Br$_2$]). The results obtained with these methods were consistent within a few percent.

Concentrations of H$_2$O and H$_2$O$_2$ in the reactor were measured in situ. The following procedure was used for the absolute calibration of the mass spectrometric signals of these species. H$_2$O was titrated with an excess of F atoms:

$$F + H_2O \rightarrow OH + HF \qquad (8)$$

$$F + OH \rightarrow O + HF \qquad (18)$$

(the FO and H atom forming channel of reaction 18 is endothermic by ≈50 kcal mol^{-1}). In this case the concentration of F atoms consumed corresponds to two times the concentration of H$_2$O: Δ[F] = 2[H$_2$O]. In turn, the concentration of F atoms was determined using titration reaction 13 in excess of Br$_2$. The concentration of F atoms could be found from the consumed fraction of Br$_2$: [F] = Δ[Br$_2$]. A procedure similar to that used for H$_2$O calibration was used for the determination of the absolute concentrations of H$_2$O$_2$. H$_2$O$_2$/H$_2$O mixture was titrated by an excess of F atoms. In this case the consumed fraction of the F atoms was due to reactions 8 and 18, and reactions 6 and 19:

$$F + HO_2 \rightarrow HF + O_2 \qquad (19)$$

The rate constant of the reaction 19 was estimated to be $k_{19} = 8.3 \times 10^{-11}$ cm^3 molecule^{-1} s^{-1} at $T = 300$ K.[15] Thus, Δ[F] =

Results

Reaction Br + HO$_2$ → HBr + O$_2$ (1). The rate constant of the reaction between Br atoms and HO$_2$ radicals was measured by monitoring the kinetics of HO$_2$ consumption with an excess of Br. Experiments were carried out in the temperature range between 230 and 355 K. The configuration used for the introduction of the reactants into the reactor is shown in Figure 1. It has to be noted that inlets 1, 2, and 3 were moved simultaneously, i.e., both Br and HO$_2$ sources were moved relative to the main reactor. The initial concentration of HO$_2$ was in the range (0.6–1.5) × 10^{12} molecule cm^{-3}; the range of Br concentrations is shown in Table 1. H$_2$O$_2$ was present in the reactor at concentrations in the range (0.6–2.5) × 10^{13} molecule cm^{-3}. Flow velocities in the reactor were 900–1450 cm s^{-1}. The consumption of the excess reactant, Br atoms, was always less than a few percent. Examples of HO$_2$ decay for different concentrations of Br atoms are shown in Figure 3. Figure 2 shows the dependence of the pseudo-first-order rate constant, $k'_1 = -d(\ln[HO_2])/dt$, as a function of Br concentration, which was measured at room temperature using different methods for HO$_2$ detection (see previous section). Examples of pseudo-first-order plots observed at different temperatures are presented in Figure 4. All pseudo-first-order rate constants, k'_1, were corrected for axial and radial diffusion of HO$_2$.[19] The diffusion coefficient of HO$_2$ in He was calculated from that of O$_2$ in He.[20]
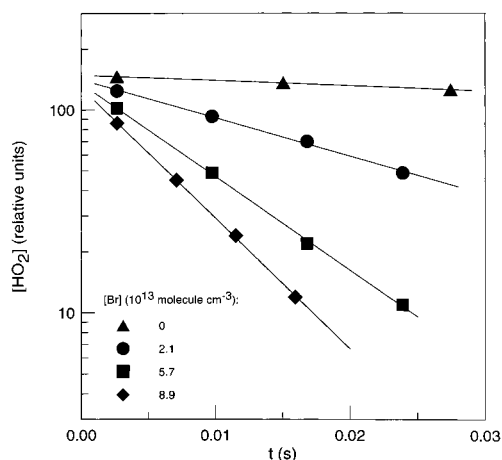
Figure 3. Reaction $Br + HO_2 \rightarrow HBr + O_2$: examples of experimental HO_2 decay kinetics monitored in excess of Br atoms at $T = 297$ K.
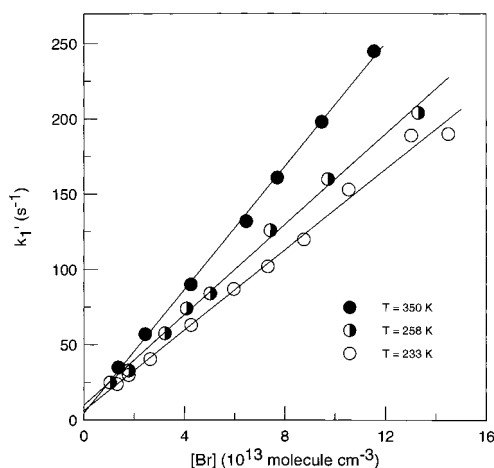

Figure 4. Reaction $Br + HO_2 \rightarrow HBr + O_2$: examples of pseudo-first-order plots obtained from HO_2 decay kinetics in excess of Br atoms.
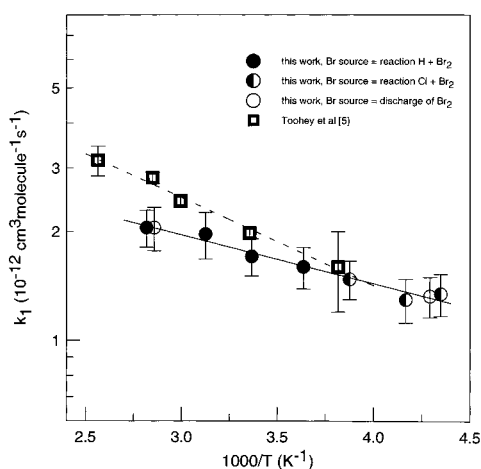

Figure 5. Reaction $Br + HO_2 \rightarrow HBr + O_2$: temperature dependence of the rate constant.

The maximal correction was 9%. The values of k_1 were obtained from the slope of the linear least-squares fit to the experimental data, as shown in Figures 2 and 4. The zero-intercepts, $3-10$ s^{-1}, were in good agreement with the rates of HO_2 decay, $6-8$ s^{-1}, measured in the absence of Br atoms for all the temperatures of the study. All of the results obtained for k_1 at the different temperatures are given in Table 1. These results are also shown in Figure 5 together with the data obtained by Toohey et al. in the unique previous temperature dependent study of reaction

TABLE 2: Reaction $Br + DO_2 \rightarrow DBr + O_2$: Experimental Conditions and Results

no/exp.[a]	T (K)	[Br] (10^{14} molecule cm^{-3})	k_3 (10^{-13} cm^3 molecule^{-1} s^{-1})[b]
8	355	0.2−1.4	4.3 ± 0.6
9	325	0.2−1.6	3.8 ± 0.5
7	295	0.1−1.2	3.0 ± 0.4
10	270	0.2−1.6	2.5 ± 0.3
10	250	0.1−1.5	2.3 ± 0.3
10	230	0.1−1.5	1.9 ± 0.3

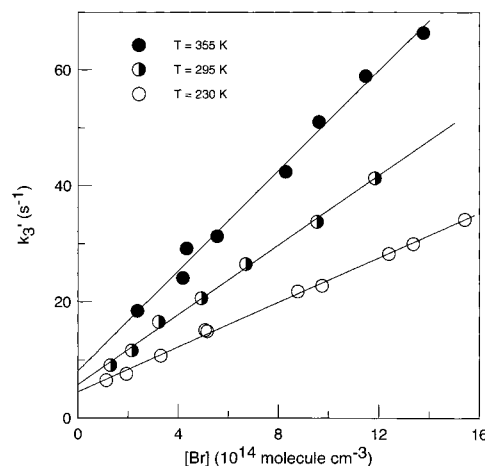[a] Number of kinetic runs. [b] Quoted uncertainty represents $1\sigma + 10\%$.

Figure 6. Reaction $Br + DO_2 \rightarrow DBr + O_2$: examples of pseudo-first-order plots obtained from DO_2 decay kinetics in excess of Br atoms.

1.[5] On the basis of a least-squares fit of the present data, we derive the following Arrhenius expression:

$$k_1 = (4.9 \pm 0.7) \times 10^{-12} \exp[-(310 \pm 40)/T]$$
$$\text{cm}^3 \text{ molecule}^{-1} \text{ s}^{-1} \qquad T = 230-355 \text{ K}$$

where the uncertainties represent 2σ.

Reaction $Br + DO_2 \rightarrow DBr + O_2$ (3). Reaction 3 has been studied in the same way as the $Br + HO_2$ reaction. Experiments were carried out under pseudo-first-order conditions using an excess of Br atoms over DO_2 radicals. The initial concentration of DO_2 radicals was in the range $(5-10) \times 10^{11}$ molecule cm^{-3} and that of Br atoms was varied between 0.1 and 1.6×10^{14} molecule cm^{-3} (Table 2). The concentration of D_2O_2 in the reactor was in the range $(3-6) \times 10^{12}$ molecule cm^{-3}. Gas flow velocity was between 700 and 1100 cm s^{-1}. The concentration of the excess reactant, Br atoms, was constant along the reaction zone. The DO_2 loss rate, measured in the absence of Br atoms, was in the range $3-6$ s^{-1} and independent of temperature. Zero-intercepts of the pseudo-first-order plots (an example is shown in Figure 6) were always in good agreement with these values, ranging from 3 to 8 s^{-1} in the whole temperature range used. As in the previous case, a diffusion correction was made on observed values of k_3', which was always lower than 4%. All of the data obtained for k_3 are given in Table 2 and shown in Figure 7. The resulting Arrhenius expression, which corresponds to the straight line in Figure 7, is

$$k_3 = (1.9 \pm 0.4) \times 10^{-12} \exp[-(540 \pm 60)/T]$$
$$\text{cm}^3 \text{ molecule}^{-1} \text{ s}^{-1} \qquad T = (230-355) \text{ K}$$
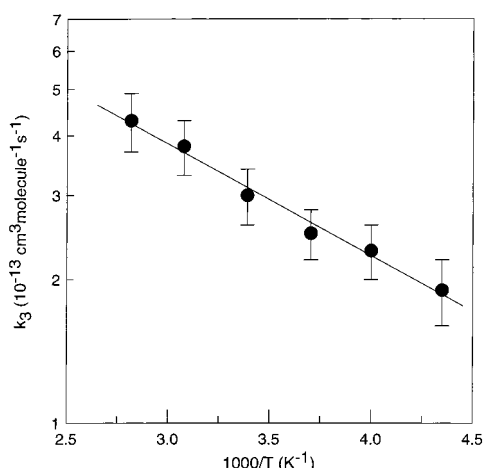
where the uncertainties are 2σ.

Figure 7. Reaction Br + DO$_2$ → DBr + O$_2$: temperature dependence of the rate constant.

TABLE 3: Reaction Br + HO$_2$ → HBr + O$_2$: Summary of Kinetic Data at *T* = 298 K

k_1 (10^{-12} cm^3 molecule^{-1} s^{-1})	method[a]	reference
0.22 ± 0.11	DF/MS	Posey et al.[2]
0.76 ± 0.09[b]	DF/MS-LIF	Poulet et al.[3]
1.98 ± 0.05[c]	DF/LMR−RF	Toohey et al.[5]
1.5 ± 0.2[d]	DF/EPR	Laverdet et al.[4]
1.7 ± 0.2[e]	DF/MS	this work

[a] DF, discharge flow system; MS, mass spectrometry; LMR, laser magnetic resonance; RF, resonance fluorescence; LIF, laser-induced fluorescence; EPR, electron paramagnetic resonance. [b] Considering new kinetic data, this value was recalculated in ref 4 to give for k_1 the range $(1.0-2.2) \times 10^{-12}$ cm^3 molecule^{-1} s^{-1}. [c] [e] Quoted uncertainties are 1σ, 2σ, and $1\sigma + 10\%$, respectively.

Discussion

The results obtained for the rate constant of the reaction Br + HO$_2$ can be compared with those from previous studies. A summary of the room-temperature data for k_1 is presented in Table 3. The value of k_1 measured in the present work agrees quite well with those from the two most recent studies.[4,5] The temperature dependence of the rate constant of reaction 1 has been studied only in one work,[5] where the following Arrhenius expression was found: $k_1 = (1.4 \pm 0.2) \times 10^{-11}$ exp[$(-590 \pm 140)/T$] cm^3 molecule^{-1} s^{-1}. These results are shown in Figure 5 together with the data from this study. In the present work, a weaker temperature dependence is found compared with the results of Toohey et al.,[5] although absolute values of k_1 can be considered as consistent within the quoted experimental uncertainties. The maximum difference between values of k_1 from these two studies, observed at highest temperature of this study (T = 355 K), is about 30%. Current evaluations of the kinetic data for atmospheric modeling[6,7] recommend a temperature dependence expression of k_1 based on the results of ref 5. Note that the Arrhenius expression from the present work results in higher values for k_1 at the temperatures of the lower stratosphere. Values higher by a factor 1.2−1.3 are found at temperatures in the range 210−230 K.

Current photochemical models, which consider HBr production only through gas-phase reactions of Br with HO$_2$ and CH$_2$O, fail to reproduce the results of recent observations of around 1−2 ppt of HBr in the altitude range 20−35 km (e.g., ref 21). These models underestimate the stratospheric concentrations of HBr. The introduction of the present kinetic data into models will lead to somewhat higher rates of HBr formation under stratospheric conditions, however, this will not change signifi-

cantly the calculated HBr profiles and, consequently, will not explain the discrepancies between measured and calculated concentrations of HBr in the stratosphere. Other unknown sources of HBr could exist. One of the potential candidates is the HBr formation in the minor channel (if it exists) of the reaction of BrO with HO$_2$ and/or OH.[8,9] This possibility is still not excluded from the most recent studies of these reactions.[6,22]

Two possible mechanisms for reaction 1 have been discussed in ref 5: a direct attack of Br at the hydrogen atom in HO$_2$ or the formation of (HOOBr)* complex with subsequent elimination of HBr and O$_2$ via a four-center transition state. The pre-exponential factors in Arrhenius expressions of k_1 have been estimated for each of these mechanisms:[5,23] $A = (0.3-1.3) \times 10^{-11}$ cm^3 molecule^{-1} s^{-1} for the Br attack on the hydrogen atom and $A = (0.2-4.2) \times 10^{-13}$ cm^3 molecule^{-1} s^{-1} in the case of a four center mechanism. Considering the value of $A = 1.4 \times 10^{-11}$ cm^3 molecule^{-1} s^{-1},[5] Toohey et al. concluded that this result was more consistent with the direct attack mechanism. The preexponential factor of k_1, $A = 4.9 \times 10^{-12}$ cm^3 molecule^{-1} s^{-1}, determined in the present study, also falls in the range $(0.3-1.3) \times 10^{-11}$ cm^3 molecule^{-1} s^{-1}, estimated for this direct H-atom transfer process.

The present determination of the rate constant for reaction 3 between Br and DO$_2$ appears to be the first one. A relatively strong kinetic isotopic effect is observed for Br + HO$_2$(DO$_2$) reactions. However, the ratio $k_1/k_3 = 5-7$, found at the temperatures of the present study, is consistent with the maximum isotope effect for H/D isotopic forms, which has been estimated to be 18.[24] This effect is due to both a lower preexponential factor and a higher activation energy for k_3. Even if a detailed quantitative analysis of this isotopic effect is beyond the scope of the present work, the present data provide a basis for theoretical calculations in order to better elucidate the mechanism of reaction 1.

References and Notes

(1) Lary, D. J. *J. Geophys. Res.* **1996**, *101*, 1505.
(2) Posey, J.; Sherwell, J.; Kaufman, M. *Chem. Phys. Lett.* **1981**, *77*, 476.
(3) Poulet, G.; Laverdet, G.; Le Bras G. *J. Chem. Phys.* **1984**, *80*, 1922.
(4) Laverdet, G.; Le Bras, G.; Mellouki, A.; Poulet, G. *Chem. Phys. Lett.* **1990**, *172*, 430.
(5) Toohey, D. W.; Brune, W. H.; Anderson, J. G. *J. Phys. Chem.* **1987**, *91*, 1215.
(6) De More, W. B.; Sander, S. P.; Golden, D. M.; Hampson, R. F.; Kurylo, M. J.; Howard, C. J.; Ravishankara, A. R.; Kolb, C. E.; Molina, M. J. *Chemical Kinetics and Photochemical Data for Use in Stratospheric Modeling*; NASA, JPL, California Institute of Technology: Pasadena, CA, 1997.
(7) Atkinson, R.; Baulch, D. L.; Cox, R. A.; Hampson, R. F.; Kerr, J. A.; Rossi, M. J.; Troe, J. *J. Phys. Chem. Ref. Data* **1997**, *26*, 521.
(8) Chipperfield, M. P.; Shallcross, D. E.; Lary, D. J. *Geophys. Res. Lett.* **1997**, *24*, 3025.
(9) Chartland, D. J.; McConnell, J. C. *Geophys. Res. Lett.* **1998**, *25*, 55.
(10) Bedjanian, Y.; Le Bras, G.; Poulet, G. *J. Phys. Chem.* **1999**, *103*, 7017.
(11) Bedjanian, Y.; Le Bras, G.; Poulet, G. *Int. J. Chem. Kinet.* **1999**, *31*, 698.
(12) Bedjanian, Y.; Riffault, V.; Le Bras, G.; Poulet, G. *J. Photochem. Photobiology A* **1999**, *128*, 15.
(13) Wada, Y.; Takayanagi, T.; Umemoto, H.; Tsunashima, S.; Sato, S. *J. Chem. Phys.* **1991**, *94*, 4896.
(14) Bedjanian, Y.; Laverdet, G.; Le Bras, G. *J. Phys. Chem.* **1998**, *102*, 953.

(15) Walther, C. D.; Wagner, H. G. *Ber. Bunsen-Ges. Phys. Chem.* **1983**, *87*, 403.

(16) Nicovich, J. M.; Wine, P. H. *Int. J. Chem. Kinet.* **1990**, *22*, 379.

(17) Bemand, P. P.; Clyne, M. A. A. *J. Chem. Soc., Faraday Trans. 2* **1976**, *72*, 191.

(18) Bedjanian, Y.; Riffault, V.; Le Bras, G.; Poulet, G. *J. Phys. Chem.*, submitted.

(19) Kaufman, F. *J. Phys. Chem.* **1984**, *88*, 4909.

(20) Morrero, T. R.; Mason, E. A. *J. Phys. Chem. Ref. Data* **1972**, *1*, 3.

(21) Nolt, I. G., et al. *Geophys. Res. Lett.* **1997**, *24*, 281.

(22) Bogan, D. J.; Thorn, R. P.; Nesbitt, F. L.; Stief, L. J. *J. Phys. Chem.* **1996**, *100*, 14838.

(23) Shum, L. G. S.; Benson, S. W. *Int. J. Chem. Kinet.* **1983**, *15*, 341.

(24) Laidler, K. J. *Chemical Kinetics*, 2nd ed.; McGraw-Hill Company: New York, 1965.